



Comparative efficiency of peanut shell and peanut shell biochar for removal of arsenic from water

Muhammad Sohail Sattar¹ · Muhammad Bilal Shakoor¹ · Shafaqat Ali¹ · Muhammad Rizwan¹ · Nabeel Khan Niazi^{2,3} · Asim Jilani⁴

Received: 29 January 2019 / Accepted: 15 April 2019 / Published online: 4 May 2019
© Springer-Verlag GmbH Germany, part of Springer Nature 2019

Abstract

Contamination of surface water and groundwater streams with carcinogenic chemicals such as arsenic (As) has been a major environmental issue worldwide, and requires significant attention to develop new and low-cost sorbents to treat As-polluted water. In the current study, arsenite (As(III)) and arsenate (As(V)) removal efficiency of peanut shell biochar (PSB) was compared with peanut shell (PS) in aqueous solutions. Sorption experiments showed that PSB possessed relatively higher As removal efficiency than PS, with 95% As(III) (at pH 7.2) and 99% As(V) (at pH 6.2) with 0.6 g L⁻¹ sorbent dose, 5 mg L⁻¹ initial As concentration, and 2 h equilibrium time. Experimental data followed a pseudo-second-order model for sorption kinetics showing the dominance of chemical interactions (surface complexation) between As and surface functional groups. The Langmuir model for sorption isotherm indicated that As was sorbed via a monolayer sorption process. The X-ray photoelectron spectroscopy (XPS) and Fourier transform infrared (FTIR) spectroscopy analyses revealed that the hydroxyl (–OH) and aromatic surface functional (C=O, C=C–C, and –C–H) groups contributed significantly in the sorption of both As species from aqueous solutions through surface complexation and/or electrostatic reactions. We demonstrate that the pyrolysis of abandoned PS yields a novel, low-cost, and efficient biochar which provides dual benefits of As-rich water treatment and a value-added sustainable strategy for solid waste disposal.

Keywords Arsenic · Biochar · Sorption · Peanut shell · XPS · Speciation

Responsible editor: Tito Roberto Cadaval Jr

Electronic supplementary material The online version of this article (<https://doi.org/10.1007/s11356-019-05185-z>) contains supplementary material, which is available to authorized users.

✉ Muhammad Bilal Shakoor
bilalshakoor88@gmail.com; bilalshakoor88@gcuf.edu.pk

¹ Department of Environmental Sciences and Engineering, Government College University Faisalabad, Faisalabad 38000, Pakistan

² Institute of Soil and Environmental Sciences, University of Agriculture Faisalabad, Faisalabad 38040, Pakistan

³ School of Civil Engineering and Surveying, University of Southern Queensland, Toowoomba, Australia

⁴ Center of Nanotechnology, King Abdulaziz University, Jeddah 21589, Saudi Arabia

Introduction

Arsenic (As) in the surface water and especially in groundwater systems is considered a threatening problem around the world. It usually occurs as arsenite (As(III)) and arsenate (As(V)) species in aqueous environments, and transformation of these two inorganic species largely depends on the aqueous pH and redox potential (Basu et al. 2014; Shakoor et al. 2017). Inorganic As forms are more toxic and mobile than those of organic As, and As(III) is considered ~60 times more toxic compared to As(V) (Shakoor et al. 2016; Taheri et al. 2017).

Groundwater contamination with As is a widespread problem around the world as people consume groundwater for their drinking, specifically in low-income countries of Southeast Asia like Pakistan and India (Raza et al. 2017; Shakoor et al. 2018a). Arsenic enrichment of groundwater resources could occur mainly through geogenic sources, for example mineral weathering processes and geothermal waters (Guo et al. 2017; Rasheed et al. 2016). Many anthropogenic/industrial sources could also discharge As into water bodies

such as smelters, mining activities, wood treatment, paints, cosmetics, pesticides, coal combustion, and highly soluble As-rich trioxide stockpiles. It has been documented that the human health is greatly affected by As poisoning, and in recent past, three major types of As-induced toxicity have been reported such as cytotoxicity, epidemiological effects, and genotoxicity (Zhou and Xi 2018).

Considering the lethal toxicity of As, the International Agency for Research on Cancer (IARC) has enlisted As in the group 1 carcinogens and forced the World Health Organization (WHO) to set the maximum limit of As in drinking water at $10 \mu\text{g L}^{-1}$ (IARC 2004; WHO 2008). Hence, to decrease As concentration below the WHO limit, the researchers have developed efficient remediation methods for the As removal from contaminated water. Previous data have shown that various technologies have been adopted for the treatment of As-rich water (Shakoor et al. 2016, 2018b).

The most widely used methods for As removal from water are ion exchange resins, coagulation, electrodialysis, reverse osmosis, and sorption using various organic and inorganic materials such as activated bauxite, activated carbon, clay, and iron (Fe) minerals (Luqman et al. 2013; Mohan et al. 2014; Shakoor et al. 2016). The treatment technologies such as reverse osmosis and ion exchange resins are costly, which restricts their large-scale application (Atar and Olgun 2007; Çolak et al. 2009). Although chemical precipitation methods using ferric/lime salts are effective, they produce secondary contamination in the form of sludge and also require maintenance cost (Atar and Olgun 2009; Cheraghi et al. 2013; Jiménez-Cedillo et al. 2013). Owing to its simplicity and reusable/regenerable nature, the sorption process has been widely applied as a preferable method to remove As from water (Olgun and Atar 2012).

In the recent 20 years, a lot of research has been done to develop and optimize inexpensive and more eco-friendly sorbents possessing similar features as activated carbons. Although As sorption has been done using agro-based sorbents, low efficiency, degradation, and coloration problems in water limited their large-scale applicability. The pretreatment/modification of sorbents may help to solve these issues and results in biopolymer ring opening, stability, high porosity, and As sorption capacity. Among the modified/pretreated sorbents, biochar has shown its suitability and applicability over the other materials (Zhou et al. 2017). Biochar is basically a solid, carbonaceous product generated by burning of organic materials in a little or no oxygen environment, and the process is called pyrolysis (Inyang et al. 2016; Khalil et al. 2018). Biochar is widely known as a multifunctional biomaterial and has largely been examined for increasing soil fertility and removal of contaminants from soil and water media (Chen et al. 2011). Recent literature has demonstrated that the use of biochar for pollutants such as heavy metal(loid) removal from aqueous solutions is highly advantageous

owing to effective surface functional moieties and great sorption capacity (Jellali et al. 2016). For instance, Inyang et al. (2012) used biochar prepared from digested dairy waste for the removal of heavy metal(loid)s from aqueous environments. Biochar produced at 450°C from wood/bark feedstock showed high removal potential of toxic heavy metal(loid)s such as cadmium (Cd), lead (Pb), and As from contaminated aqueous solutions (Mohan et al. 2007).

There are a variety of oxygen-rich surface functional groups on the surface of biochar, for example hydroxyl ($-\text{OH}$), carboxylate ($-\text{COOH}$), carbonyl ($-\text{COH}$), and amino ($-\text{NH}_2$) groups which are used to remove heavy metalloids from the wastewater (Ding et al. 2018). A great variety of abundantly available organic materials from forestry, agriculture wastes, and animal husbandry are used for the generation of low-cost biochar, and peanut shell is one of them (Ali et al. 2017; Dieme et al. 2017; Rizwan et al. 2016; Wu et al. 2017). According to the United States Department of Agriculture (USDA) in 2017, the peanut and peanut oil production was 43.39 million metric tons and 6.08 million metric tons, respectively (USDA 2017).

Peanut shell (PS) is an inexpensive, abundant, and commonly available waste in China, Pakistan, and other countries worldwide which could be used as an excellent feedstock material for the production of biochar (Cheng et al. 2016). A few studies have highlighted the efficiency of biochar produced from peanut shell for removal of toxic elements such as Pb from water (Wang et al. 2015). However, little or no attention has been paid to find out the efficiency of peanut shell biochar (PSB) for As removal from water.

To employ biochar for successful removal of As from water, it is therefore critical to examine the oxidation states of As after sorption onto sorbents using advanced techniques such as X-ray photoelectron spectroscopy (XPS). However, to our knowledge, limited data are available on the analyses of As sorption behavior on solid sorbent interface using XPS.

Therefore, the current study aims to develop PSB to (1) assess its ability for As(III) and As(V) removal at varying environmental conditions (pH, initial metalloid concentration, sorbent dose, contact time), (2) compare the isotherms and kinetics of As species sorption by PS and PSB, and (3) investigate the sorption behavior using XPS and Fourier transform infrared (FTIR) spectroscopy.

Materials and methods

Experimental materials

Sodium arsenite (NaAsO_2) and disodium hydrogen arsenate ($\text{Na}_2\text{HAsO}_4 \cdot 7\text{H}_2\text{O}$) were purchased from Sigma-Aldrich Chemical Co. (Germany) and used as a source of As(III) and As(V), respectively, in all the experiments. Standard stock

solutions (1000 mg L^{-1}) of both species of As were prepared by dissolving appropriate quantities of NaAsO_2 and $\text{Na}_2\text{HAsO}_4 \cdot 7\text{H}_2\text{O}$ salts. The experiments were conducted in triplicates.

Preparation of PS as sorbent

The PS was obtained from local market in Faisalabad. The material was air-dried, sun-dried, and kept in an oven at 70°C for 24 h. The dried PS was then ground and sieved through a $< 250\text{-}\mu\text{m}$ sieve to keep the size uniform.

Preparation and characterization of PSB

The PSB was prepared using PS as a feedstock according to the method described by Qayyum et al. (2015). In short, a manually fabricated stainless steel vertical silo-type furnace (10 kg capacity) having a gas burner was employed for the pyrolysis of PS. The flame ignited did not directly touch the PS, and the process was continued for 2 h at 450°C followed by cooling of the material (referred to as biochar) in the furnace.

The PSB was characterized for different physicochemical attributes (Table A.1 in the Supplementary Material) such as pH and electrical conductivity (EC) of biochar (1:20, *w/v*, weight-to-deionized water (DW) ratio)) were measured using pH (HM-12P; TOA Electronics, South Korea) and EC (Jenway Limited model 4070, England) meters, respectively. The volatile content and total ash of biochar were determined by burning the PSB in a muffle furnace at 450°C and 550°C , respectively. Phosphorus (P) and other metal (Ni, Zn, Cd, Pb) contents were measured using a spectrophotometer and atomic absorption spectrophotometer (novAA 350; Analytik Jena, Germany), respectively, after digesting the PSB in di-acid ($\text{HNO}_3/\text{HClO}_4$) mixture. The PSB had EC, pH, ash, moisture, mobile, and resident matter values as 2.16 dS m^{-1} , 8.01, 49.52%, 0.94%, 10.47%, and 50.47%, respectively (Table A.1 in the Supplementary Material). The values of P, Ni, Cd, Pb, and Zn were 0.15%, 18.96%, 3.13%, 5.21%, and 35.9%, respectively (Table A.1 in the Supplementary Material).

Molybdenum blue method for arsenic analysis

The concentrations of As(III) (after oxidation to As(V)) and As(V) were determined in water samples according to the molybdenum blue color method as reported by Lenoble et al. (2003), in which As concentration was analyzed by the development of an antimonyl-arsenomolybdate complex (see details in the Supplementary Material). In short, ascorbic acid solution (0.2 mL) and reagent A (0.4 mL) were added to a 10-mL test tube containing 8 mL water sample while the rest of the volume was filled using DW. A blank sample was also

made according to the procedure stated above. The reaction mixture was left for 60 min at room temperature ($20^\circ\text{C} \pm 2^\circ\text{C}$) to form complex and blue color development before analysis using a UV-visible double-beam spectrophotometer (Dynamica Halo DB-20, UK) set at 870 nm (Lenoble et al. 2003).

Sorption experiments

Effect of pH

Standard stock solution of 1000 mg L^{-1} was used to add required concentration (5 mg L^{-1}) of As(III) and As(V) in the working solutions. The 0.1 M NaCl solution was used as a background electrolyte to retain a constant ionic strength during the experiments. About 0.015 g of PS and PSB was added to 25 mL of As(III) and As(V) working solutions having varying pH values to equalize a 0.6 g L^{-1} sorbent dose. The pH of the working solutions was adjusted to 3, 4, 5, 6, 7, 8, 9, and 10 by employing the HCl or NaOH (0.1 M each) solutions. The samples were shaken (at 20°C) for 2 h on an orbital shaker set at 120 rpm, centrifuged, filtered ($0.45\text{-}\mu\text{m}$ membrane), and stored to analyze As by using a spectrophotometer as described above.

The equilibrium As concentration (mg g^{-1}) sorbed per unit weight of sorbents (PS and PSB) (q_e) was assessed by Eq. (1) (Prasad et al. 2014)

$$q_e = \frac{(C_o - C_e) V}{m} \quad (1)$$

where C_o and C_e (mg L^{-1}) refer to original and equilibrium concentrations, respectively, while m (g) and V (L) mean the sorbent mass (g).

The percent As removal from samples was obtained by Eq. (2) (Prasad et al. 2014)

$$\% \text{As removal} = \frac{C_o - C_e}{C_o} \times 100 \quad (2)$$

where C_o and C_e (mg L^{-1}) have been defined above.

Sorption kinetics

To determine the optimum time for maximum sorption of As, kinetic studies were carried out at around 20°C temperature. Approximately 0.015 g (0.6 g L^{-1}) of PS and PSB was added to 25 mL of working solutions containing an optimum concentration (5 mg L^{-1}) of As(III) and As(V); the solution pH was set (based on pH study) at 7.2 and 5.4 for As(III) and As(V) sorption, respectively, by using HCl or NaOH (0.01 M each) solutions. The samples were then shaken at 120 rpm on an orbital shaker for different contact time periods which ranged from 0.016 to 24 h. Filtered samples were used

to determine As by using a spectrophotometer as described above. Kinetic data were subjected to non-linear kinetic models such as pseudo-first-order and pseudo-second-order models to explore the rate of both As species on PS and PSB. The governing equations used for kinetic modeling are described below (Ghorbani-Khosrowshahi and Behnajady 2016):

$$\text{Pseudo-first order : } q_t = q_e(1 - e^{-k_1 t}) \quad (3)$$

$$\text{Pseudo-second order : } q_t = \frac{q_e^2 k_2 t}{1 + q_e k_2 t} \quad (4)$$

where q_e and q_t (mg g^{-1}) mean As sorbed at equilibrium time and any time t , respectively, and k_1 (min^{-1}) and k_2 ($\text{g mg}^{-1} \text{min}^{-1}$) are the rate constants for pseudo-first-order and pseudo-second-order models.

Sorption isotherms

The effect of initial concentration of both As species was assessed by using varying concentrations of As(III) and As(V). The sorbent dose of 0.015 g (0.6 g L^{-1}) of PS and PSB was added to 25 mL of working solutions containing different concentrations of both As species ($0.01\text{--}7 \text{ mg L}^{-1}$). The pH of As(III) working solutions was set at 7.2 while 5.4 for As(V) using HCl or NaOH (0.1 M each) solutions, and samples were shaken for 2 h at 120 rpm on an orbital shaker. Arsenic in the filtered samples was measured by using a spectrophotometer as described above. The mechanism of As sorption onto PS and PSB was determined by fitting the isotherm, equilibrium data to four different non-linear isotherm models, and the detail of the modeling is described in the Supplementary Material.

Effect of sorbent dose

The optimum sorbent dose was determined, and experiments were conducted at 5 mg L^{-1} initial sorbate concentration, 2 h contact time, and 7.2 (As(III)) and 5.4 (As(V)) pH levels. Various sorbent doses, i.e., 0.1 g L^{-1} , 0.3 g L^{-1} , 0.6 g L^{-1} , 0.9 g L^{-1} , 1 g L^{-1} , and 1.3 g L^{-1} , were applied, and As concentration in filtrate solution was analyzed using a spectrophotometer as described above.

Quality assurance and quality control

The chemicals and solutions used for all the experiments were analytical grade. All the glassware/plasticware used in the current study was thoroughly washed with 2% HNO_3 solution followed by rinsing (twice) with DW. To check the precision and accuracy during the analyses of As in stored samples, the

samples of known As values such as $10 \text{ } \mu\text{g L}^{-1}$, $30 \text{ } \mu\text{g L}^{-1}$, and $40 \text{ } \mu\text{g L}^{-1}$ were also analyzed after each ten As samples.

Surface characterization

The surface characterization (survey scans and chemical states) of PS and PSB before and after As loading was done by PHI 5000 Versa Probe II XPS under ultra-high vacuum ($\sim 10^{-7}$ mbar). The survey spectrum of PS and PSB was obtained from 0 to 1100 eV, and XPS data was interpreted using Multipack software (Ver. 9; ULVAC-PHI, Inc., Japan). The specific surface functional groups of PS and PSB were analyzed using FTIR spectroscopy, and the infrared spectra of PS and PSB were acquired in the wavenumber range of $400\text{--}4000 \text{ cm}^{-1}$.

Results and discussion

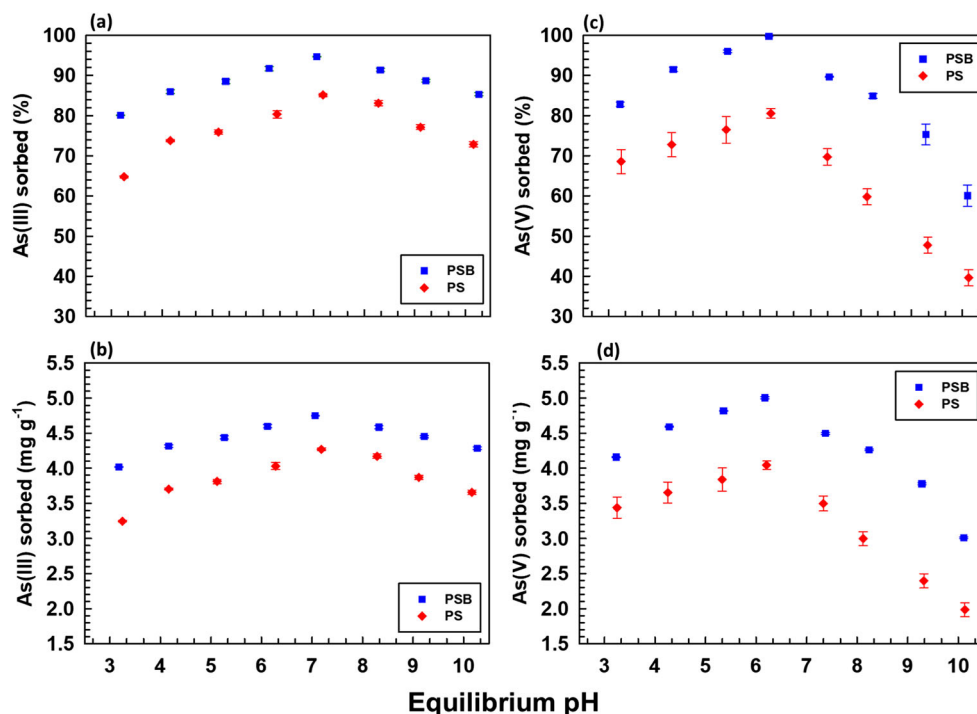
Influence of pH

Figure 1a, b shows that As(III) removal was dependent upon the solution pH, because, initially, an increasing trend was observed for As(III) sorption reaching to a maximum sorption at 7.1 and 7.2 near neutral pH for PS (4.27 mg g^{-1} and 85%) and PSB (4.75 mg g^{-1} , 95%), respectively. A further increase in pH significantly reduced the sorption of both PS and PSB. In the case of As(V), sorption increased gradually until the equilibrium was achieved at pH 6.2—both for PS (4.04 mg g^{-1} and 81%) and PSB (5.01 mg g^{-1} and 99%), respectively, after which reduction in sorption was obvious as shown in Fig. 1c, d. The PSB displayed more As sorption compared to PS for both species of As (10% As(III) and 18% As(V), respectively), and notably more As(V) (4%) was removed by PSB compared to As(III) while PS showed higher As(III) (4%) removal than As(V).

Arsenic(III) species mainly occurs as a neutral (H_3AsO_3) species in the pH range of 2 to 9 (Samsuri et al. 2013), whereas above pH 9, it predominates as an anionic $\text{H}_2\text{AsO}_3^{3-}$ species (Niazi et al. 2018a, 2018b). The sorption behavior of As(III) onto PS and PSB in this experiment was nearly the same as reported on Japanese oak wood and perilla leaf biochars, where authors found the highest As(III) sorption (3.2 mg g^{-1} and 1.81 mg g^{-1}) at pH around 7–8 (Niazi et al. 2018a, 2018b). In this sorption experiment, maximum As(III) removal around a neutral pH (7.1) value might be associated with the less or no competition between negatively charged surface functional groups ($-\text{OH}$, $-\text{COOH}$) and neutral species of As (H_3AsO_3) which could otherwise happen under acidic pH (6) or alkaline pH (7.5) in water (Abid et al. 2016; Zhang et al. 2018).

The As(V) species such as H_2AsO_4^- and HAsO_4^{2-} dominate in the solution under the pH range (3–10) ($\text{p}K_1 = 2.2$, $\text{p}K_2$

Fig. 1 a–d Effect of different solution pH levels on As sorption by peanut shell and peanut shell biochar. Experimental conditions: temperature of 20 °C, initial As concentration of 5 mg L⁻¹, contact time of 2 h, and sorbent dose of 0.6 g L⁻¹



= 6.98) tested here (Boddu et al. 2008; Wu et al. 2017). Low pH is more suitable for successful protonation of sorbent surface, leading to the development of positively charged sorption sites, and facilitates the electrostatic interactions between anionic species of As and biosorbent surface, thereby yielding maximum As removal (Zhou et al. 2017). Relatively higher As(V) removal from water at acidic pH for PSB could be due to reduced aromaticity and increased surface polarity after pyrolysis, thus producing more acidic functional groups on PSB compared to PS, thereby favoring As(V) binding with positively charged surface of PSB via electrostatic attraction (Niazi et al. 2018a, 2018b).

At the high pH range, negatively charged sorption sites increase and repulsive forces exist between sorbent surface and As anions; consequently, As(V) sorption declines progressively (García-Rosales et al. 2018). The declining sorption with rising pH values (> 7.2) could also be linked with the competition between negatively charged functional groups (–OH, –COOH) with As(V) anions (Zhang et al. 2018). Moreover, PSB possessed additional functional groups on the surface which enhanced its porosity, thus removing more As species compared to PS.

Sorption kinetics

The contact time used for the experiments ranged from 0.016 to 24 h to obtain the equilibrium. The sorption rate of As species was fast initially, with As(III) removal of 70% and 90% by PS and PSB, respectively, while 81% and 97% of As(V) removal was achieved by PS and PSB, respectively,

at 2 h contact time (Fig. 2). A further increase in sorption time had a minimum effect on sorption of As species by PS and PSB.

Both PS and PSB removed up to 9% more As(V) compared to As(III) and PSB proved more efficient in removing As(V) than PS with 16% more As(V) removal capacity. The sorption occurred swiftly until 2 h, achieving equilibrium and slowed down thereafter. In the past, such kinetic behavior has been ascribed to the rapid development of outer-sphere complexes initially and, after which, inner-sphere complexes are formed gradually (Ding et al. 2018). High loading of As species decreased the uptake capacity of both PS and PSB, and this loading effect might also be explained partially by dilution,

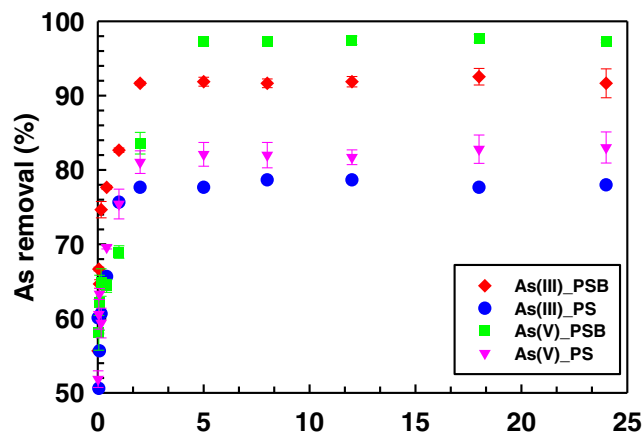


Fig. 2 Removal of As from aqueous solutions using peanut shell and peanut shell biochar as a function of contact time (0.016–24 h). Experimental conditions: temperature of 20 °C, initial As concentration of 5 mg L⁻¹, and sorbent dose of 0.6 g L⁻¹

Table 1 Non-linear kinetic modeling parameters of As sorption onto peanut shell and peanut shell biochar for As removal from aqueous solutions

Biosorbent	Pseudo-first-order model			Pseudo-second-order model		
	q_e (mg g ⁻¹)	k_1 (min ⁻¹)	R^2	q_e (mg g ⁻¹)	k_2 (g mg ⁻¹ min ⁻¹)	R^2
As(III)						
Peanut shell	2.96 ± 0.08	17.85 ± 3.73	0.93	3.04 ± 0.05	9.60 ± 1.47	0.97
Peanut shell biochar	3.52 ± 0.1	24.23 ± 5.24	0.94	3.61 ± 0.06	11 ± 2.35	0.98
As(V)						
Peanut shell	3.90 ± 0.12	27.09 ± 7.62	0.91	4.09 ± 0.09	10.12 ± 0.02	0.95
Peanut shell biochar	4.60 ± 0.16	25.47 ± 7.94	0.88	4.76 ± 0.13	7.51 ± 2.44	0.95

as As is adsorbed onto sorbents, its concentration in solution reduces, hence less As sorption with increasing contact time (Shakoor et al. 2018b; Yoon et al. 2017).

The sorption kinetic data were fitted to nonlinear pseudo-first-order and pseudo-second-order models to delineate mononuclear and binuclear sorption (Figure A.1 in the Supplementary Material). Table 1 shows kinetic models' parameter values for As sorption data. The comparison of models based on R^2 values elucidated that the kinetic data of both As species were best fitted with pseudo-second-order (R^2 = up to 0.98) for PS and PSB (Table 1). However, a slightly higher R^2 value was obtained from the pseudo-second-order model applied to kinetic data of PSB (0.98) compared to PS (0.97) in the case of As(III).

The results explain that the amount of surface sorption sites on PS and PSB could partially influence the rate of sorption, and the rate-determining step could probably be owing to chemisorption which involved the chemical interactions (e.g., surface complexation) between As oxyanions and surface functional groups (Mohan et al. 2011).

Sorption isotherm

The sorption isotherm studies were conducted to examine the sorption potential of both As species by PS and PSB at the initial metalloid concentration of 0.01–7 mg L⁻¹ (Figure A.2 in the Supplementary Material). The maximum sorption of As(III) and As(V) at the current experimental setup was observed as 3.10 mg g⁻¹ and 2.74 mg g⁻¹ by PS, respectively, while PSB sorbed more As than PS which was 3.92 mg g⁻¹ (As(III)) and 3.15 mg g⁻¹ (As(V)) with a 4–5 mg L⁻¹ initial metalloid concentration (Figure A.2 in the Supplementary Material). A further increase in the concentration of As (up to 7 mg L⁻¹) caused minimum/negligible improvement in the sorption of both As species on PS and PSB. In this study, the highest As sorption was obtained at relatively lower initial metalloid concentrations (4–5 mg L⁻¹) which could be inferred to enlarge surface area and availability of more accessible binding sites for As (Tajernia et al. 2014).

The experimental data were computed with nonlinear isotherm models of Langmuir, Freundlich, Temkin, and Dubinin–Radushkevich (Figure A.3a–d in the Supplementary Material) as described in the Supplementary Material. The model values for all four models are shown in Table 2. First, in the Freundlich isotherm model, the parameter n for both As species was < 1, As(III) (0.27 and 0.32) and As(V) (0.32), which assumes that the sorption process is favorable on PS and PSB (Table 2). The correlation coefficients (R^2) of Langmuir isotherm (As(III) [0.97, 0.98] and As(V) [0.98, 0.99]) are comparatively higher than those obtained from the Freundlich model (As(III) [0.94, 0.96] and As(V) [0.90, 0.96]) (Fig. 3a–d). These results suggest that monolayer sorption governed by surface complexation and electrostatic interactions between As(III)/As(V) and surface functional groups dominated the process in both experiments conducted using PS and PSB, but slightly higher R^2 values were obtained from isotherm data of PSB than PS.

The Langmuir separation factors (R_L) were extracted to test the favorability of sorption (Figure A.4a, b in the Supplementary Material). The results showed that R_L values were < 1, indicating favorable sorption of both As species onto PS and PSB.

The Temkin isotherm model described higher R^2 values for As(V) removal than As(III) by both the sorbents (Figure A.3a–d in the Supplementary Material). The heat of sorption (b) values were 0.37 and 0.95 for As(III) sorption on PS and PSB, respectively, while for As(V), the values were reported as 0.38 and 0.48 for PS and PSB, respectively (Table 2). This indicated that a linear reduction in b values caused the maximum coverage of both species of As on PS and PSB (Foo and Hameed 2010).

In the case of the Dubinin–Radushkevich model, again higher R^2 values for As(V) removal were extracted than for As(III) by both the sorbents (Figure A.3a–d in the Supplementary Material).

Among all the models, the Langmuir model provided the best fit (confirmed by the highest R^2 values up to 0.99) to isotherm data of both species of As, suggesting that the monolayer process was involved in As sorption onto PS and PSB.

Table 2 Non-linear isotherm modeling parameters of As sorption onto peanut shell and peanut shell biochar for As removal from aqueous solutions

Biosorbent	Langmuir ^a		Freundlich ^a		Temkin ^a		Dubinin-Redushkevich ^a		R^2			
	Q_L (mg g ⁻¹)	K_L (L g ⁻¹)	R^2	Q_F (mg ¹⁻ⁿ g ⁻¹ L ⁻ⁿ)	1/n	R^2	A	R^2		Q_D (mg g ⁻¹)	E (kJ g ⁻¹)	
As(III)												
Peanut shell	11.21 ± 1.32	3.17 ± 0.9	0.97	2.40 ± 0.18	0.27 ± 0.02	0.94	0.37 ± 0.01	897.28 ± 3.4	0.82	4.10 ± 1.22	0.08 ± 0.004	0.91
Peanut shell biochar	7.60 ± 1.32	1.62 ± 0.50	0.98	2.23 ± 0.12	0.32 ± 0.07	0.96	0.95 ± 0.01	23.66 ± 4.40	0.95	5.10 ± 1.23	0.07 ± 0.001	0.98
As(V)												
Peanut shell	11.31 ± 1.12	3.17 ± 0.72	0.98	1.90 ± 0.55	0.32 ± 0.09	0.90	0.38 ± 0.23	210 ± 40.21	0.83	2.64 ± 1.41	0.02 ± 0.002	0.92
Peanut shell biochar	7.94 ± 1.11	2.17 ± 0.23	0.99	2.23 ± 0.16	0.32 ± 0.8	0.96	0.48 ± 0.21	152.30 ± 17	0.91	3.1 ± 1.11	0.07 ± 0.002	0.97

Influence of sorbent dose

The effect of sorbent dose was determined to optimize the quantity of sorbent needed for the maximum removal of As (Figure A.5a, b in the Supplementary Material). The results showed that there was a substantial increase in As(III)/As(V) removal with the increasing dose of sorbents. The maximum sorption was obtained at 0.6 g L⁻¹ for both species of As by PS and PSB, but notably PS and PSB (82% and 93%, respectively) removed more As(V) compared to As(III) (68% and 88%, respectively) from aqueous solutions after which a declining trend was observed. The low As removal at a high dose of sorbents could be due to the presence of unsaturated binding cavities which indicates that the number of sorption sites increases with the addition of high dosage but fixed initial metalloid concentration causes reduction in the sorption (Kumar et al. 2011; Lalmunsiana and Lee 2012).

Surface characterization

FTIR analysis

The FTIR spectra of PS and PSB before and after As(III)/As(V) sorption are shown in Fig. 3a–f, which identified the functional groups present on the surface of sorbents and their interaction with As species, i.e., As(III)/As(V).

FTIR spectra of PS

In the case of PS, the broad and strong band before As sorption at 3225 cm⁻¹ was attributed to the typical presence of hydroxyl (–OH), and the band observed at 2852 cm⁻¹ can be nominated to –CH₂ stretching on sorbent (Fig. 3a) (Liu et al. 2017). The peak at 1636 cm⁻¹ was assigned to the stretching vibration of the asymmetrical carboxyl group (–COOH). The small peak observed at 1522 cm⁻¹ was described to the ether group (Fig. 3a).

After As(III) and As(V) sorption, there were shifts to a lower and higher side as a result of the As(III) or As(V) sorption in –OH, –CH₂, and –COOH at about 3275 cm⁻¹, 2860 cm⁻¹, and 1624 cm⁻¹ for As(III), while at 3280 cm⁻¹, 2867 cm⁻¹, and 1624 cm⁻¹ in the case of As(V) (Fig. 3b, c). We conclude that specific functional groups (–OH, –CH₂, and –COOH) contributed to sorption of both As species; however, –OH showed considerable shifts in the peaks compared to other functional groups and thus strongly adsorbed As(III) or As(V) through an ion exchange mechanism (Ahmad et al. 2013; Shakoor et al. 2018b).

FTIR spectra of PSB

Figure 3e, f represents the FTIR spectra of PSB and As(III) and As(V) loaded PSB. For PSB, the spectral band at 3618

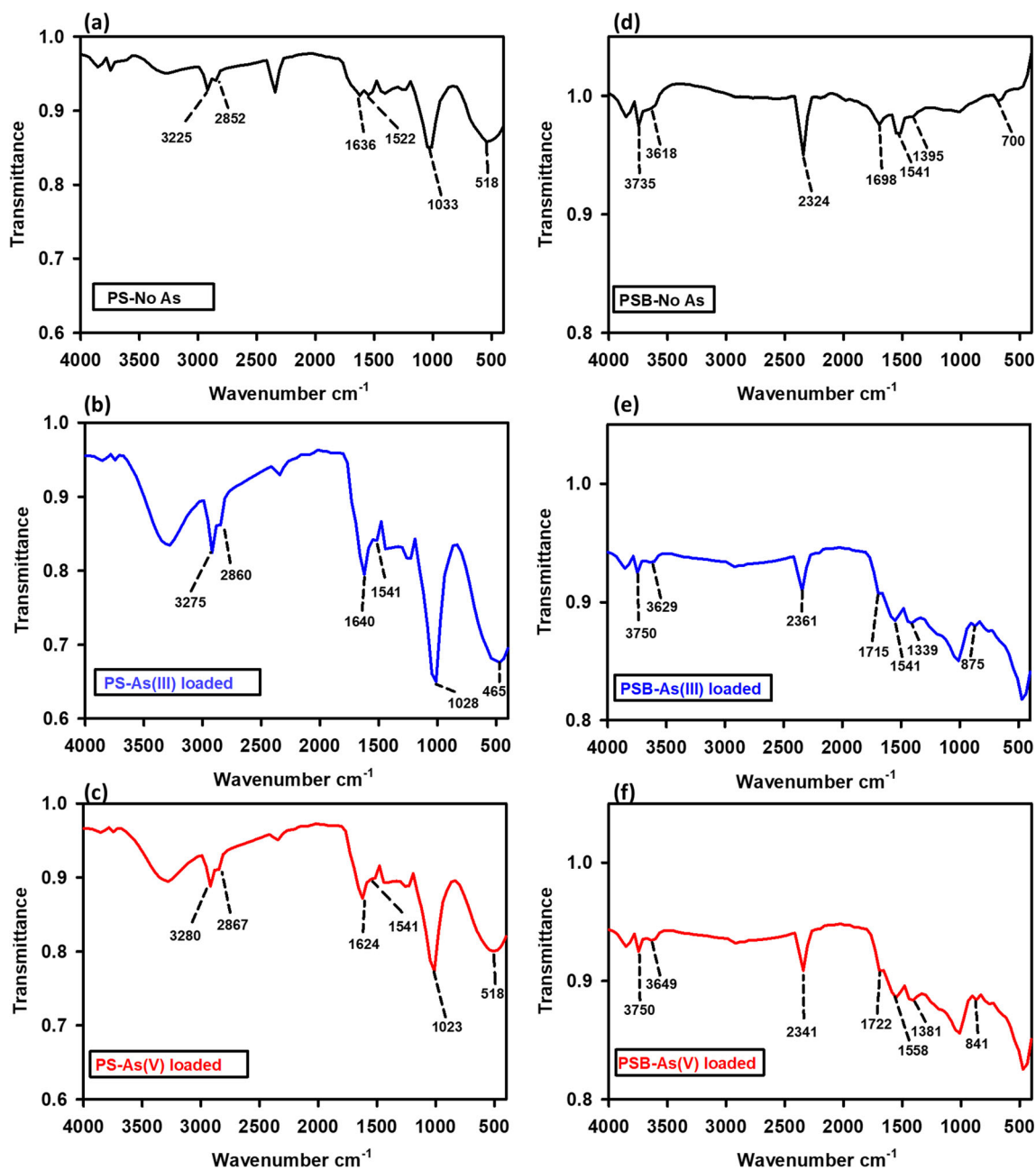


Fig. 3 The FTIR spectra of peanut shell and peanut shell biochar before (a, d) and after (b, e) As(III) and c, f As(V) sorption

cm^{-1} was characteristics of the -OH group present in phenols or alcohol (R-k et al. 2011). The spectral peak, although small, at 1698 cm^{-1} could be due to the stretching vibration of C=O bonds of the nonionic carboxyl groups (-COOH , -COOCH_3) and may be linked to carboxylic acids and/or their ester groups (Abid et al. 2016; Mohan et al. 2014). Under an oxygen-deficient environment and at high temperature ($450 \text{ }^\circ\text{C}$), thermal cracking occurs in pyrolysis of biomass, which produces both the volatile matters and improves the quantity of aromatic surface functional groups (Fang et al. 2013) through dehydrogenation of carbohydrates followed by condensation process (Cope et al. 2014; Niazi et al. 2018a). Two peaks at 1541

cm^{-1} and 1395 cm^{-1} were nominated to aromatic C=C and/or C=C-C vibrations while, at 700 cm^{-1} , described to aromatic -C-H out-of-plane stretching (El-Banna et al. 2018; Keiluweit et al. 2010). On the whole, our results demonstrated that unlike PS, the surface of As-unloaded PSB was mainly occupied by aromatic surface functional groups (Fig. 3) (Dong et al. 2011).

After As or As(III) and As(V) loading, some substantial changes in FTIR spectral bands of PSB were prominent (Fig. 3e, f). The -OH , C=O , C=C-C , and -C-H stretching bands at 3618 cm^{-1} , 1698 cm^{-1} , 1395 cm^{-1} , and 700 cm^{-1} , respectively, were shifted to 3629 cm^{-1} , 1715 cm^{-1} , 1339

cm^{-1} , and 875 cm^{-1} for As(III) and to 3649 cm^{-1} , 1722 cm^{-1} , 1381 cm^{-1} , and 841 cm^{-1} after As(V) sorption, suggesting the chemical interactions such as surface complexation/precipitation and electrostatic interactions had occurred between the As(III) or As(V) and surface functional groups (Prakash et al. 2013).

The findings of this study highlight that As(III) and As(V) probably occupied the sorption cavities in the FTIR spectral region in which –OH groups largely dominated for both PS and PSB and thus adsorb As on their surface complexation and electrostatic interactions (Niazi et al. 2018b; Vithanage et al. 2017). In addition, for PSB aromatic C=O, C=C–C and

–C–H surface functional groups also played a significant role in As uptake from contaminated water (Mohan et al. 2014; Niazi et al. 2018a). However, future research work should be focused to analyze the distinct linkage between As(III)/As(V) with biochar which caused shifts in the spectral bands after As loading reported in the current study.

XPS spectra

The XPS survey scans of PS and PSB before and after As(III) or As(V) sorption are shown in Figs. 4 and 5 as well as in the Supplementary Material (Figures A.6 and A.7). The results

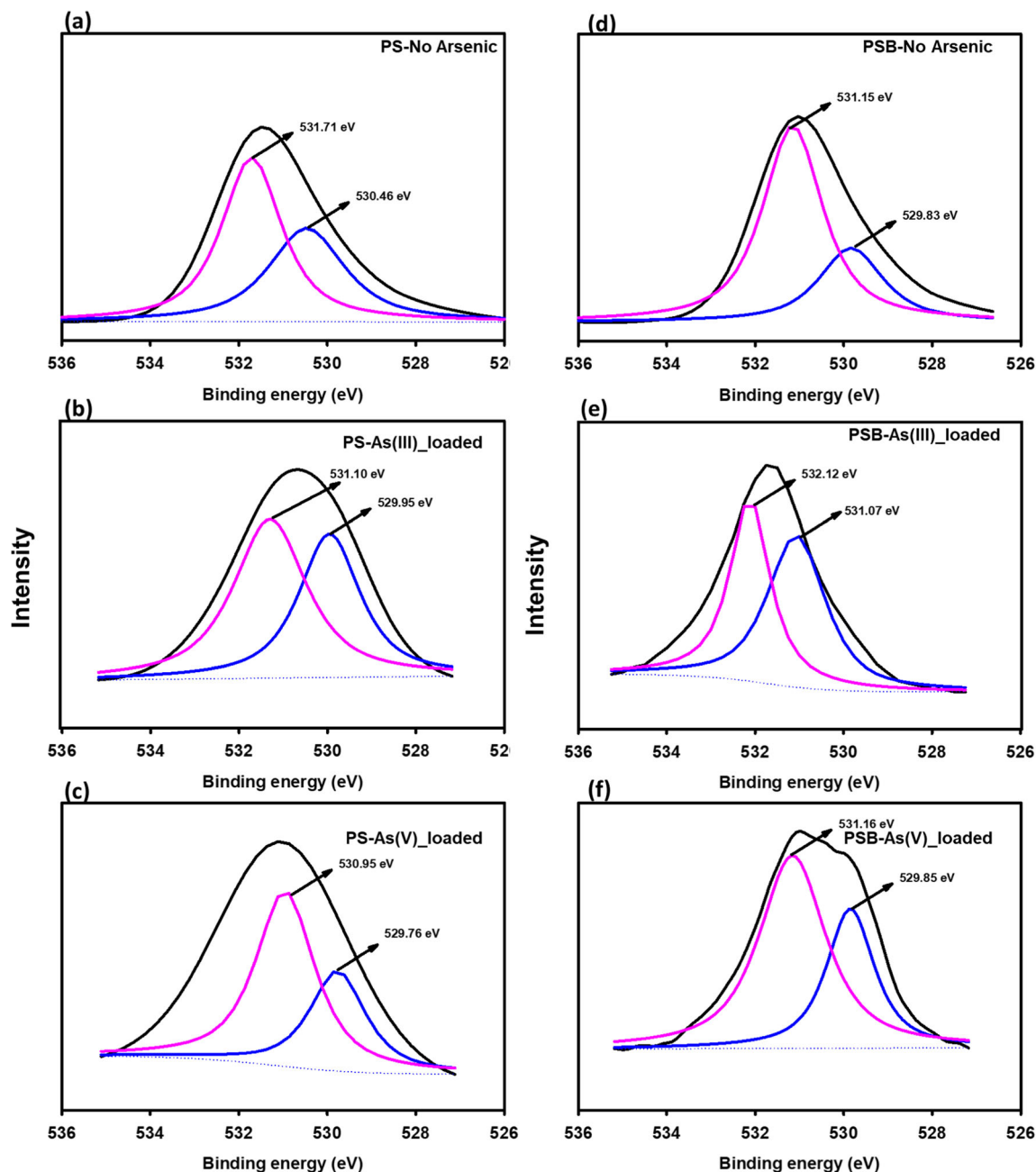


Fig. 4 The O1s XPS spectra of peanut shell and peanut shell biochar before (a, d) and after (b, e) As(III) and c, f As(V) sorption

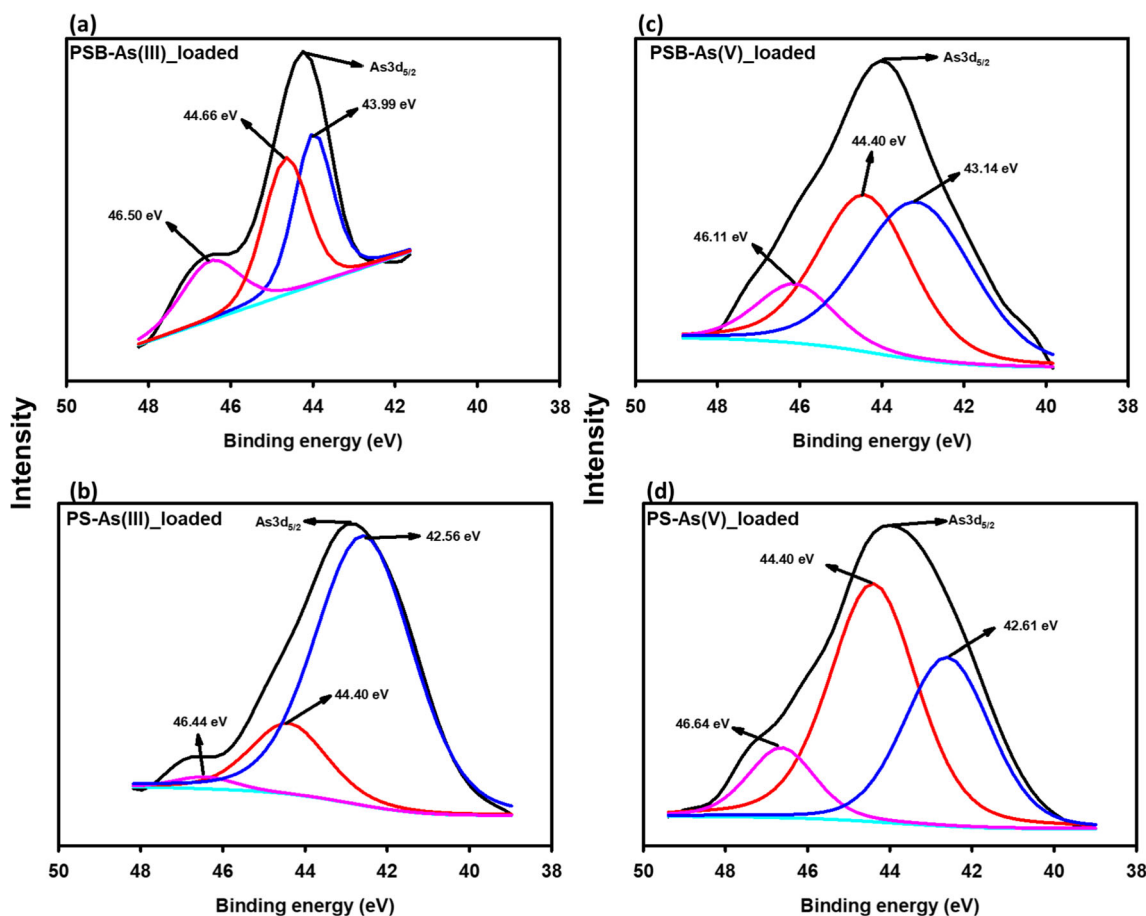


Fig. 5 The As3d XPS spectra of peanut shell and peanut shell biochar after (a, b) As(III) and (c, d) As(V) sorption

showed that carbon (C) (75.4%, 20.2%) and oxygen (O) (82.2%, 16.4%) were dominant elements in the surface composition of PS and PSB, respectively (Figures A.7 and A.8 in the Supplementary Material). After As(III) sorption, the percentage of sorbed As(III) was observed as < 0.1% and 0.5% on PS and PSB, respectively, while As(V)-loaded PS and PSB showed 0.5% and 0.6% of As(V), respectively (Figures A.6 and A.7 in the Supplementary Material). The percentage of As(V) sorbed was slightly higher on PS and PSB compared to As(III), showing greater potential of removing As(V) than As(III) by both sorbents.

The XPS spectra of O1s for PS and PSB indicated that the surface of the sorbents was enriched with O-containing surface functional groups (Fig. 4a–f). There are two energy peaks at 531.71 eV and 530.46 eV for PS and at 531.15 eV and 529.83 eV for PSB which were assigned to O=C–O and carbonyl (O=C) groups, respectively (Fig. 4a–f) (López et al. 1991). After As(III) sorption, the change in binding energy was prominent at 531.16 eV (PS) and 532.12 eV (PSB) in the case of O=C–O while at 529.85 eV (PS) and 531.07 eV (PSB) which represented the carbonyl group (Fig. 4b–e).

Similarly, As(V)-loaded PS and PSB showed an increase/decrease in binding energy at 530.95 eV (PS) and 531.16 eV

(PSB), indicating O=C–O, and at 529.76 eV (PS) and 529.85 eV (PSB) for the carbonyl group (Fig. 4c–f). It is obvious from the results that O-rich –O=C–O and O=C surface functional groups had big devotion to As and sorbed both As species through electrostatic interactions (Zhou et al. 2017).

High-resolution XPS spectra of As-loaded PS and PSB in the As3d region are shown in Fig. 5a–d. It is reported that 3d binding energy was about 45.5 eV for As(V) in Na₂HAsO₄, 44.2 eV for As(III) in NaAsO₂, and 41.5 eV for As(0), respectively (Hu et al. 2015). Therefore, 44.40 eV and 44.66 eV of As3d binding energy showed the presence of As(III) while 46.64 eV and 46.11 eV confirmed As(V) sorption on the surface of PS and PSB, respectively.

Table A.2 in the Supplementary Material compares the sorption potential of sorbents examined in the current study with previous studies. In this study, PSB showed higher sorption capacity for both As species, i.e., 4.75 mg g⁻¹ (As(III)) and 5.01 mg g⁻¹ (As(V)), compared to the various sorbents evaluated previously (Table A.2). It is suggested that PSB has great potential to be used as an efficient sorbent to remove both As species from aqueous streams.

Conclusions

The conversion of PS into PSB significantly enhanced the physiochemical characteristics and successfully removed the higher As(V) (5.01 mg g^{-1} , 99%) concentration at pH 6.2 than As(III) (4.75 mg g^{-1} , 95%) at pH 7.2 from contaminated water. The XPS and FTIR analysis revealed that PSB possessed some additional surface functional groups such as C=O, C=C–C, and –C–H which increased the As(III) and As(V) removal potential of PSB than PS. The kinetic study revealed that As(III)/As(V) removal by PS and PSB followed the pseudo-second-order model which was controlled by the chemisorption process. The Langmuir model provided the best fit to isotherm data and showed highly favorable monolayer As(III)/As(V) sorption onto PS and PSB. Moreover, both surface complexation and electrostatic interactions between As and PSB contributed to the sorption of As(III)/As(V), according to the results of adsorption envelop (pH study), modeling, and FTIR and XPS analysis. In brief, the results of this study showed that the novel PSB as a biosorbent provided a new environmentally friendly and cost-effective opportunity for As removal (specially As(V)) from contaminated water streams.

Acknowledgements The authors thank the Center of Nanotechnology, King Abdulaziz University, Jeddah, Saudi Arabia, for providing the analytical facility.

Funding information The study received financial support from the Higher Education Commission (HEC), Pakistan (Project No. 1430/SRGP/R&D/HEC/2016) and Government College University Faisalabad, Pakistan. Dr Nabeel Khan Niazi is thankful to the University of Agriculture Faisalabad and University of Southern Queensland, Australia.

References

- Abid M, Niazi NK, Bibi I, Farooqi A, Ok YS, Kunhikrishnan A, Ali F, Ali S, Igalavithana AD, Arshad M (2016) Arsenic (V) biosorption by charred orange peel in aqueous environments. *Int J Phytoremediation* 18:442–449
- Ahmad M, Lee SS, Rajapaksha AU, Vithanage M, Zhang M, Cho JS, Lee S-E, Ok YS (2013) Trichloroethylene adsorption by pine needle biochars produced at various pyrolysis temperatures. *Biomagn Res Technol* 143:615–622
- Ali S, Rizwan M, Qayyum MF, Ok YS, Ibrahim M, Riaz M, Arif MS, Hafeez F, Al-Wabel MI, Shahzad AN (2017) Biochar soil amendment on alleviation of drought and salt stress in plants: a critical review. *Environ Sci Pollut Res* 24:12700–12712
- Atar N, Olgun A (2007) Removal of acid blue 062 on aqueous solution using calcinated colemanite ore waste. *J Hazard Mater* 146:171–179
- Atar N, Olgun A (2009) Removal of basic and acid dyes from aqueous solutions by a waste containing boron impurity. *Desalination* 249:109–115
- Basu A, Saha D, Saha R, Ghosh T, Saha B (2014) A review on sources, toxicity and remediation technologies for removing arsenic from drinking water. *Res Chem Intermed* 40:447–485
- Boddu VM, Abburi K, Talbott JL, Smith ED, Haasch R (2008) Removal of arsenic (III) and arsenic (V) from aqueous medium using chitosan-coated biosorbent. *Water Res* 42:633–642
- Chen B, Chen Z, Lv S (2011) A novel magnetic biochar efficiently sorbs organic pollutants and phosphate. *Bioresour Technol* 102:716–723
- Cheng Q, Huang Q, Khan S, Liu Y, Liao Z, Li G, Ok YS (2016) Adsorption of Cd by peanut husks and peanut husk biochar from aqueous solutions. *Ecol Eng* 87:240–245
- Cheraghi M, Lorestani B, Merrikhpour H, Mosaed HP (2013) Assessment efficiency of tea wastes in arsenic removal from aqueous solution. *Desal Water Treat*:1–6
- Çolak F, Atar N, Olgun A (2009) Biosorption of acidic dyes from aqueous solution by *Paenibacillus macerans*: kinetic, thermodynamic and equilibrium studies. *Chem Eng J* 150:122–130
- Cope CO, Webster DS, Sabatini DA (2014) Arsenate adsorption onto iron oxide amended rice husk char. *Sci Total Environ* 488:554–561
- Dieme M, Villot A, Gerente C, Andres Y, Diop S, Diawara C (2017) Sustainable conversion of agriculture wastes into activated carbons: energy balance and arsenic removal from water. *Environ Technol* 38:353–360
- Ding Z, Xu X, Phan T, Hu X, Nie G (2018) High adsorption performance for As (III) and As (V) onto novel aluminum-enriched biochar derived from abandoned Tetra Paks. *Chemosphere* 208:800–807
- Dong X, Ma LQ, Li Y (2011) Characteristics and mechanisms of hexavalent chromium removal by biochar from sugar beet tailing. *J Hazard Mater* 190:909–915
- El-Banna MF, Mosa A, Gao B, Yin X, Ahmad Z, Wang H (2018) Sorption of lead ions onto oxidized bagasse-biochar mitigates Pb-induced oxidative stress on hydroponically grown chicory: experimental observations and mechanisms. *Chemosphere* 208:887–898
- Fang Q, Chen B, Lin Y, Guan Y (2013) Aromatic and hydrophobic surfaces of wood-derived biochar enhance perchlorate adsorption via hydrogen bonding to oxygen-containing organic groups. *Environ Sci Technol* 48:279–288
- Foo K, Hameed B (2010) Insights into the modeling of adsorption isotherm systems. *Chem Eng J* 156:2–10
- García-Rosales G, Longoria-Gándara L, Cruz-Cruz G, Olayo-González M, Mejía-Cuero R, Pérez PÁ (2018) Fe-TiOx nanoparticles on pineapple peel: synthesis, characterization and As (V) sorption. *Environ Nanotechnol Monit Manag* 9:112–121
- Ghorbani-Khosrowshahi S, Behnajady M (2016) Chromium (VI) adsorption from aqueous solution by prepared biochar from *Onopordom Heteracanthom*. *Int J Environ Sci Technol* 13:1803–1814
- Guo H, Zhang D, Ni P, Cao Y, Li F (2017) Hydrogeological and geochemical comparison of high arsenic groundwaters in inland basins, PR China. *Proced Earth Plan Sc* 17:416–419
- Hu X, Ding Z, Zimmerman AR, Wang S, Gao B (2015) Batch and column sorption of arsenic onto iron-impregnated biochar synthesized through hydrolysis. *Water Res* 68:206–216
- IARC (2004) Some drinking-water disinfectants and contaminants, including arsenic. *IARC Monogr Eval Carcinog Risks Hum* 84:1–477
- Inyang M, Gao B, Yao Y, Xue Y, Zimmerman AR, Pullammanappallil P, Cao X (2012) Removal of heavy metals from aqueous solution by biochars derived from anaerobically digested biomass. *Bioresour Technol* 110:50–56
- Inyang MI, Gao B, Yao Y, Xue Y, Zimmerman A, Mosa A, Pullammanappallil P, Ok YS, Cao X (2016) A review of biochar as a low-cost adsorbent for aqueous heavy metal removal. *Crit Rev Environ Sci Technol* 46:406–433
- Jellali S, Diamantopoulos E, Haddad K, Anane M, Dumer W, Mlayah A (2016) Lead removal from aqueous solutions by raw sawdust and magnesium pretreated biochar: experimental investigations and numerical modelling. *J Environ Manag* 180:439–449
- Jiménez-Cedillo MJ, Olguin MT, Fall C, Colin-Cruz A (2013) As(III) and As(V) sorption on iron-modified non-pyrolyzed and pyrolyzed

- biomass from *Petroselinum crispum* (parsley). *J Environ Manag* 117:242–252
- Keiluweit M, Nice PS, Johnson MG, Kleber M (2010) Dynamic molecular structure of plant biomass-derived black carbon (biochar). *Environ Sci Technol* 44:1247–1253
- Khalil U, Shakoor MB, Ali S, Rizwan M (2018) Tea waste as a potential biowaste for removal of hexavalent chromium from wastewater: equilibrium and kinetic studies. *Arab J Geosci* 11:573
- Kumar J, Balomajumder C, Mondal P (2011) Application of agro-based biomasses for zinc removal from wastewater—a review. *CLEAN – Soil, Air, Water* 39:641–652
- Lalhmunsiam DT, Lee S-M (2012) Activated carbon and manganese coated activated carbon precursor to dead biomass in the remediation of arsenic contaminated water. *Environ Eng Res* 17:41–48
- Lenoble V, Deluchat V, Serpaud B, Bollinger J-C (2003) Arsenite oxidation and arsenate determination by the molybdene blue method. *Talanta* 61:267–276
- Liu S, Xu W-h, Y-g L, X-f T, G-m Z, Li X, Liang J, Zhou Z, Z-l Y, X-x C (2017) Facile synthesis of Cu (II) impregnated biochar with enhanced adsorption activity for the removal of doxycycline hydrochloride from water. *Sci Total Environ* 592:546–553
- López GP, Castner DG, Ratner BD (1991) XPS O 1s binding energies for polymers containing hydroxyl, ether, ketone and ester groups. *Surf Interface Anal* 17:267–272
- Luqman M, Javed MM, Yasar A, Ahmad J, Khan A (2013) An overview of sustainable techniques used for arsenic removal from drinking water in rural areas of the Indo-Pak subcontinent. *Soil and Environ* 32:87–95
- Mohan D, Pittman CU Jr, Bricka M, Smith F, Yancey B, Mohammad J, Steele PH, Alexandre-Franco MF, Gomez-Serrano V, Gong H (2007) Sorption of arsenic, cadmium, and lead by chars produced from fast pyrolysis of wood and bark during bio-oil production. *J Colloid Interface Sci* 310:57–73
- Mohan D, Rajput S, Singh VK, Steele PH, Pittman CU Jr (2011) Modeling and evaluation of chromium remediation from water using low cost bio-char, a green adsorbent. *J Hazard Mater* 188:319–333
- Mohan D, Sarswat A, Ok YS, Pittman CU Jr (2014) Organic and inorganic contaminants removal from water with biochar, a renewable, low cost and sustainable adsorbent—a critical review. *Bio. Res. Technol.* 160:191–202
- Niazi NK, Bibi I, Shahid M, Ok YS, Burton ED, Wang H, Shaheen SM, Rinklebe J, Luttge A (2018a) Arsenic removal by perilla leaf biochar in aqueous solutions and groundwater: an integrated spectroscopic and microscopic examination. *Environ Pollut* 232:31–41
- Niazi NK, Bibi I, Shahid M, Ok YS, Shaheen SM, Rinklebe J, Wang H, Murtaza B, Islam E, Nawaz MF (2018b) Arsenic removal by Japanese oak wood biochar in aqueous solutions and well water: investigating arsenic fate using integrated spectroscopic and microscopic techniques. *Sci Total Environ* 621:1642–1651
- Olgun A, Atar N (2012) Equilibrium, thermodynamic and kinetic studies for the adsorption of lead (II) and nickel (II) onto clay mixture containing boron impurity. *J Ind Eng Chem* 18:1751–1757
- Prakash O, Singh SK, Singh B, Singh RK (2013) Investigation of coordination properties of isolated adenine to copper metal: a systematic spectroscopic and DFT study. *Spectrochim Acta A Mol Biomol Spectrosc* 112:410–416
- Prasad KS, Ramanathan A, Paul J, Subramanian V, Prasad R (2014) Biosorption of arsenite (As^{+3}) and arsenate (As^{+5}) from aqueous solution by *Arthrobacter* sp. biomass. *Environ Technol* 34:2701–2708
- Qayyum MF, Abid M, Danish S, Saeed MK, Ali MA (2015) Effects of various biochars on seed germination and carbon mineralization in an alkaline soil. *Pakistan J Agric Sci* 51:977–982
- Rasheed H, Slack R, Kay P (2016) Human health risk assessment for arsenic: a critical review. *Crit Rev Environ Sci Technol* 46:1529–1583
- Raza M, Hussain F, Lee J-Y, Shakoor MB, Kwon KD (2017) Groundwater status in Pakistan: a review of contamination, health risks, and potential needs. *Crit Rev Environ Sci Technol*:1–50
- Rizwan M, Ali S, Qayyum MF, Ibrahim M, Zia-ur-Rehman M, Abbas T, Ok YS (2016) Mechanisms of biochar-mediated alleviation of toxicity of trace elements in plants: a critical review. *Environ Sci Pollut Res* 23:2230–2248
- R-k X, S-c X, Yuan J-h, A-z Z (2011) Adsorption of methyl violet from aqueous solutions by the biochars derived from crop residues. *Bioresour Technol* 102:10293–10298
- Samsuri AW, Sadeq-Zadeh F, Seh-Bardan BJ (2013) Adsorption of As (III) and As (V) by Fe coated biochars and biochars produced from empty fruit bunch and rice husk. *J Environ Chem Eng* 1:981–988
- Shakoor MB, Niazi NK, Bibi I, Murtaza G, Kunhikrishnan A, Seshadri B, Shahid M, Ali S, Bolan NS, Ok YS, Abid M, Ali F (2016) Remediation of arsenic-contaminated water using agricultural wastes as biosorbents. *Crit Rev Environ Sci Technol* 46:467–499
- Shakoor MB, Nawaz R, Hussain F, Raza M, Ali S, Rizwan M, Oh S-E, Ahmad S (2017) Human health implications, risk assessment and remediation of As-contaminated water: a critical review. *Sci Tot Environ* 601:756–769
- Shakoor MB, Bibi I, Niazi NK, Shahid M, Nawaz MF, Farooqi A, Naidu R, Rahman MM, Murtaza G, Luttge A (2018a) The evaluation of arsenic contamination potential, speciation and hydrogeochemical behaviour in aquifers of Punjab, Pakistan. *Chemosphere* 199:737–746
- Shakoor MB, Niazi NK, Bibi I, Shahid M, Sharif F, Bashir S, Shaheen SM, Wang H, Tsang DC, Ok YS (2018b) Arsenic removal by natural and chemically modified water melon rind in aqueous solutions and groundwater. *Sci Total Environ* 645:1444–1455
- Taheri M, Gharraie MHM, Mehrzad J, Afshari R, Datta S (2017) Hydrogeochemical and isotopic evaluation of arsenic contaminated waters in an argillic alteration zone. *J Geochem Explor* 175:1–10
- Tajemia H, Ebadi T, Nasernejad B, Ghafori M (2014) Arsenic removal from water by sugarcane bagasse: an application of response surface methodology (RSM). *Water Air Soil Pollut* 225:1–22
- USDA (2017) <https://apps.fas.usda.gov/psdonline/circulars/oilseeds.pdf>.
- Vithanage M, Herath I, Joseph S, Bundschuh J, Bolan N, Ok YS, Kirkham M, Rinklebe J (2017) Interaction of arsenic with biochar in soil and water: a critical review. *Carbon* 113:219–230
- Wang Z, Liu G, Zheng H, Li F, Ngo HH, Guo W, Liu C, Chen L, Xing B (2015) Investigating the mechanisms of biochars removal of lead from solution. *Bioresour Technol* 177:308–317
- WHO (2008): Guidelines for drinking-water quality. T, pp. 306
- Wu C, Huang L, Xue S-G, Huang Y-Y, Hartley W, M-q C, Wong M-H (2017) Arsenic sorption by red mud-modified biochar produced from rice straw. *Environ Sci Pollut Res* 24:18168–18178
- Yoon K, Cho D-W, Tsang DC, Bolan N, Rinklebe J, Song H (2017) Fabrication of engineered biochar from paper mill sludge and its application into removal of arsenic and cadmium in acidic water. *Bioresour Technol* 246:69–75
- Zhang W, Liu C, Zheng T, Ma J, Zhang G, Ren G, Wang L, Liu Y (2018) Efficient oxidation and sorption of arsenite using a novel titanium (IV)-manganese (IV) binary oxide sorbent. *J Hazard Mater* 353:410–420
- Zhou Q, Xi S (2018) A review on arsenic carcinogenesis: epidemiology, metabolism, genotoxicity and epigenetic changes. *Regul Toxicol Pharmacol* 99:78–88
- Zhou Z, Y-g L, S-b L, H-y L, G-m Z, X-f T, C-p Y, Ding Y, Z-l Y, X-x C (2017) Sorption performance and mechanisms of arsenic (V) removal by magnetic gelatin-modified biochar. *Chem Eng J* 314:223–231